International Journal of Engineering

Journal Homepage: www.ije.ir

Investigating the Effect of Soil Layering on Soil-structure Interaction under Seismic Load

M. Zarinfar*

Department of Civil Engineering, Bu-Ali Sina University, Hamedan, Iran

PAPER INFO

Paper history:
Received 24 April 2022
Received in revised form 05 July 2022
Accepted 07 July 2022

Keywords:
Rock Layer
Seismic Analysis
Steel Moment
Soft Soil
Soil and Structure Interaction

ABSTRACT

Considering soil layering is a crucial and effective issue in investigating the seismicity of structures. However, previous studies have not examined the presence of a rock layer in soft soil. So, in the present paper, the effect of the rock layer in soft soil on the forces and displacements created in the low-and mid-rise steel moment frame was investigated. Thus, several numerical calculations were performed on 12 different sizes of rock layers at three different depths. Finite element models were analyzed using ABAQUS Software and considering the interaction of structure and soil. Results of the studies showed that the value of force and displacement depends on the frequency of the structure, the frequency of the soil-structure system, dominant earthquake frequency, the rock weight, and the stiffness of the structure. Two new parameters are defined that have a linear relationship with force and displacement. Results show that the thickness and length of the rock layer affect the value of force and displacement. Also, the presence of a rock layer in the soil may not be reliable and may increase the shear force by up to 27%, the axial force by up to 10%, and the moment by up to 19%. The effect of the presence of a rock layer on the displacement is more than on the force and increases the lateral displacement by up to 31% and the relative vertical displacement of the foundation by up to 59%.

doi: *10.5829/ije.2022.35.10a.17*

1. INTRODUCTION

The damage to artificial structures caused by earthquakes has long been a matter of concern, and earthquakes of different intensities significantly impact human production and life [1, 2]. Macroseismic vulnerability and seismic damage are important issues in the field of seismic safety. Vulnerability analysis of typical structures has been studied in the literature [3-5].

Without considering the interaction of structure and soil, dynamic structure analysis will not correspond to reality. The movement transmitted from the earthquake to the structure depends not only on the characteristics of the earthquake, the earthquake route, and the local conditions of the site but also on the interaction of soil and structure. The presence of soil increases the acceleration of the earthquake transmitted to the structure and increases the flexibility of the structure [6]. The first factor is the cause of more seismic damage in structures built on soft soil than in structures built on hard soil, so that the performance of the structure may change from the life-safe to a near-collapse without considering the interaction of the structure and the soil [7, 8]. The second factor reduces the frequency of the soil-structure system. Propagating waves from the structure increase the damping of the soil-structure system because of the radiation of energy in the soil [6].

Past studies on the structure and soil interaction were analytical [9], numerical [7, 10], and laboratory [11]. Aydin et al. [12] investigated the influence of soil-structure interaction on the optimal design of damping devices. The structure and soil interaction can be ignored for flexible structures built on hard soils. However, in the presence of stiff structures on soft soils, the interaction has particular importance and should be considered in the analysis of the structure. This issue has been shown by Kim and Roesset [13] by analyzing the system of one degree of freedom and by other researchers by analyzing

*Corresponding Author Institutional Email: zarinfar@basu.ac.ir (M. zarinfar)

Please cite this article as: M. Zarinfar, Investigating the Effect of Soil Layering on Soil-structure Interaction under Seismic Load, ***International Journal of Engineering, Transactions A: Basics***, Vol. 35 No. 10, (2022), 1989-2006

the structure of the moment frame [10]. Fatahi et al. [14] showed that the lateral displacement of the structure and the period of the soil-structure system increase with increasing bedrock depth. Tabatabaiefar et al. [10] showed that ignoring the interaction does not necessarily lead to the design of safe moment frames with moderate height. For the structures built on soft soil, the motion transmitted to the structure is different from the free field movement because the structure and soil interaction create additional dynamic deformation [8]. Mostly by considering the structure and soil interaction, the base shear will decrease, and the storey displacement will increase.

Although several studies have been conducted on the soil and structure interaction, the effect of the presence of a rock layer in soft soil has not been examined. The importance of including soil layering in seismic analysis has been reported in past studies. Damages reported from the Northridge Earthquake in 1994 indicate that soil layering can affect the dynamic response of the entire system [15]. Rayhani and El Naggar [16] examined the impact of soil profile thickness, soil layering, buried depth of the structure, and lateral boundary distance on the results of soil and structure interaction analysis. They showed that considering an equivalent layer could not provide an accurate prediction of reality, and soil layering should be considered in the analysis. Past studies have not been referred to the size of the rock layer and how it affects the force and displacement created in the structure under the effect of the earthquake. The aim of this article is to investigate the effect of the presence of the rock layer in soft soil on the force and displacement created in the structure by considering the interaction of soil and structure. For this purpose, the results of numerical modeling with shaking table experiments presented in the study conducted by Hokmabadi et al. [8] and Tabatabaiefar et al. [10] were first compared. Then, the rock layers were modeled in 12 different sizes, at three depths, and under three steel moment frames with different heights in ABAQUS Software. By applying records of the Kobe earthquake (near-field earthquake) and El Centro earthquake (far-field earthquake), the value of axial force, shear force, moment, and displacement in the structure are calculated, and the effect of the rock layer on the results is analyzed.

2. NUMERICAL MODEL VALIDATION

The shaking table test mentioned in the studies conducted by Hokmabadi et al. [8] and Tabatabaiefar et al. [10] was used to validate the model. In the two papers, they used dynamic similarities to scale the earthquake record. The advantage of using dynamic similarity in experiments is that the same value of gravity acceleration and density are considered in reality and the model. However, other parameters such as time, force, acceleration, etc., should be used in a scaled manner. The scaled records of the El Centro and Kobe earthquakes are shown in Figures 1 and 2. Experiments were performed on the structure fixed to the shaking table and the structure built on the shallow foundation to examine the impact of soil-structure interaction.

The width of the structure is 0.4 m, the height of the structure is 1.5 m, and the number of the storey is 15. The shear wave velocity in the soil is 36 m per second. Not only the shear wave velocity in the soil must be scaled, but also the soil bearing capacity must also be sufficient. For this purpose, a combination of kaolinite, bentonite, lime, and volcanic ash was used in these articles. More details on the way of performing the experiment and the parameters used to model the soil and structure can be found in the mentioned articles.

The time history of horizontal acceleration at the 15th storey obtained from a two-dimensional plane strain analysis for a structure fixed to the shaking table and a structure placed on the soil by applying a scaled El Centro earthquake is shown in Figures 3 and 4. The results obtained for the lateral displacement of the 15th storey as a result of applying the scaled Kobe earthquake are shown in Figures 5 and 6. The value of lateral

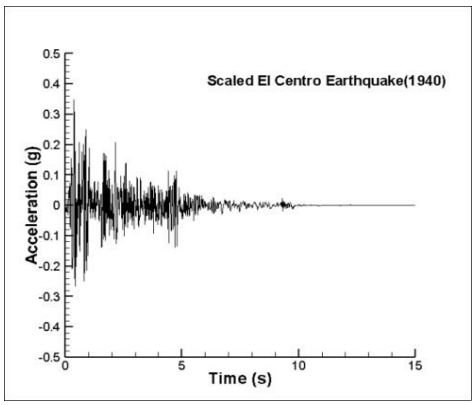

Figure 1. The scaled El Centro earthquake record

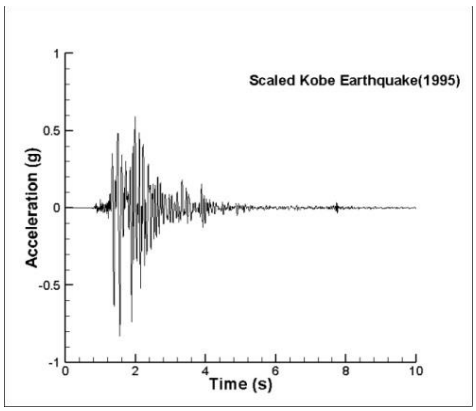

Figure 2. The scaled Kobe earthquake record

displacement is obtained by deducting the shaking table motion from the lateral displacement of the stories. The maximum lateral displacement of the stories measured in the laboratory by applying the El Centro earthquake and the value estimated by the numerical model are presented in Figure 7.

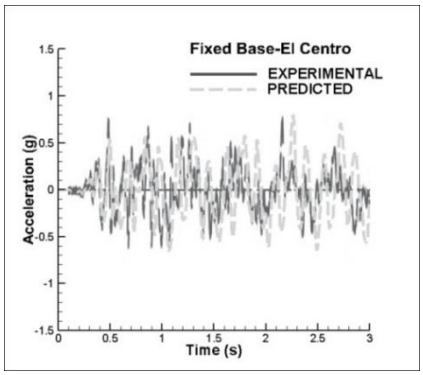

Figure 3. Time-history acceleration at the roof level of the structure under the El Centro earthquake for the fixed-base structure

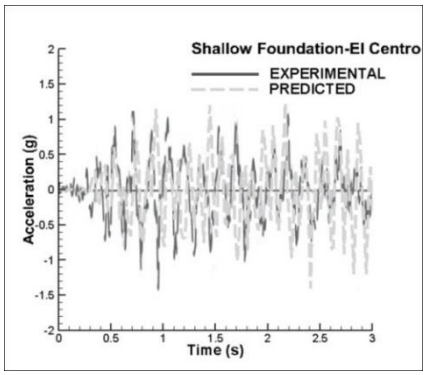

Figure 4. Time-history acceleration at the roof level of the structure under the El Centro earthquake for the structure with shallow foundation

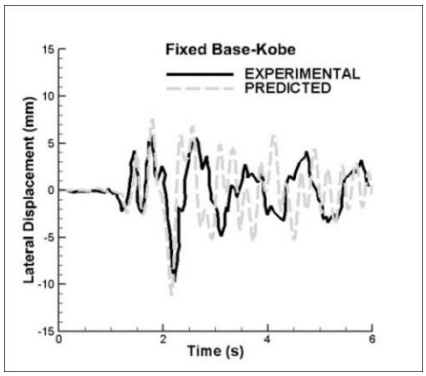

Figure 5. Time-history displacement at the roof level of the structure under the Kobe earthquake for the fixed-base structure

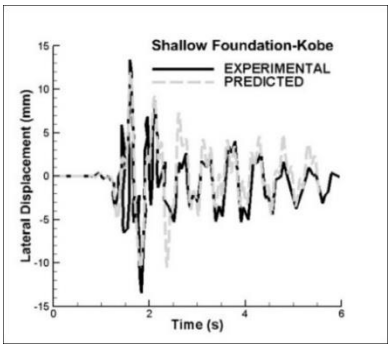

Figure 6. Time-history displacement at the roof level of the structure under the Kobe earthquake for the structure with shallow foundation

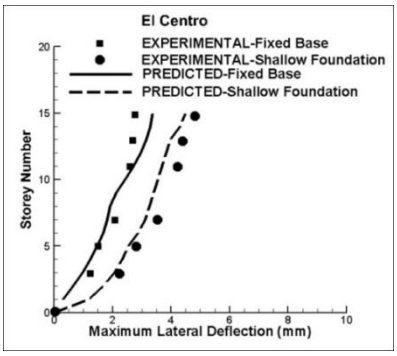

Figure 7. Comparison of experimental and numerical predictions of maximum lateral displacements

There is a good agreement between the results obtained from the laboratory and the numerical analysis, which includes the history of lateral displacement, lateral acceleration, and maximum lateral displacement of the stories in terms of trend and value. Since; the analyses are performed in the structure with a fixed base and the structure on the soil, this numerical analysis can be used as an alternative to the structure and soil system for further studies.

The next simulation includes the soil-structure model problem illustrated by Zienkiewicz et al. [17]. Homogeneous soil properties are assumed, and the incoming seismic wave is considered El Centro. The comparison of displacement, acceleration, and stress histories of control points indicates the validity of the numerical simulations (Figures 8 to 13).

3. MODEL DESCRIPTION AND ASSUMPTIONS

In this section, the effect of the rock layer in soft soil on the force and lateral displacement created in the low-and mid-rise steel structures is examined. For this purpose, the interaction of steel moment frames of 6-, 9- and 12-storey and soft clay was considered. The characteristics of the studied frames are shown in Table 1.

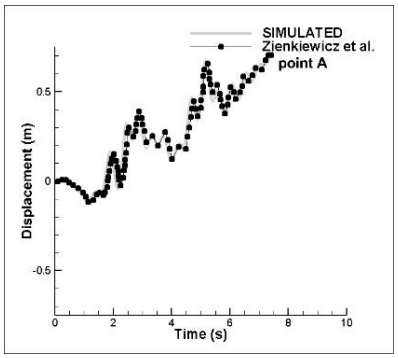

Figure 8. Comprision of displacement history at point A

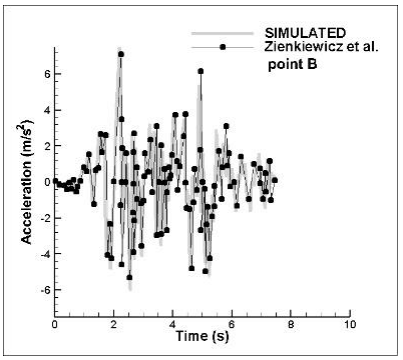

Figure11. Comprision of acceleration history at point B

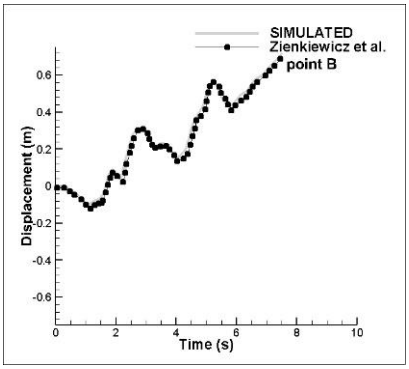

Figure 9. Comprision of displacement history at point B

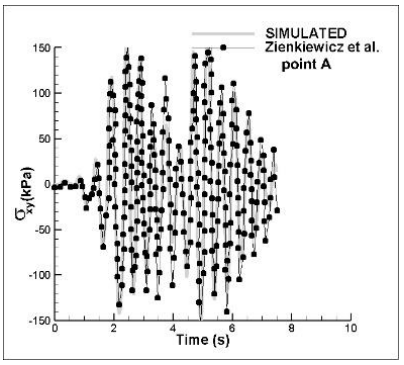

Figure 12. Comprision of stress history at point A

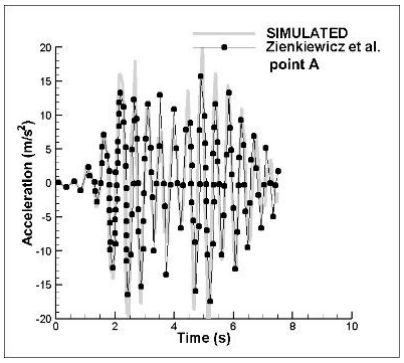

Figure 10. Comprision of acceleration history at point A

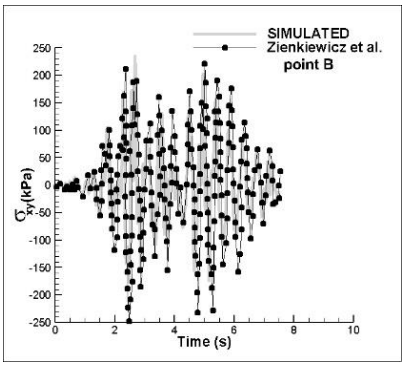

Figure 13. Comprision of stress history at point B

The characteristics of the numerical models, for the 12-storey structure include the location of the bedrock, the dimensions of the structure, and the soil medium are shown in Figure 14. The numerical models of 6- and 9-storey structures are constructed in exactly the same way. In this paper, it is assumed that the bedrock is located at a depth of 30 m below the soil surface. The results presented by Rayhani and El Naggar [16] show that the

TABLE 1. Characteristics of the steel frames

Name	Number of stories	Number of bays	Storey height (m)	Bay width (m)	Total height (m)	Total width (m)
S6	6	3	3	3	18	9
S9	9	3	3	3	27	9
S12	12	3	3	3	36	9

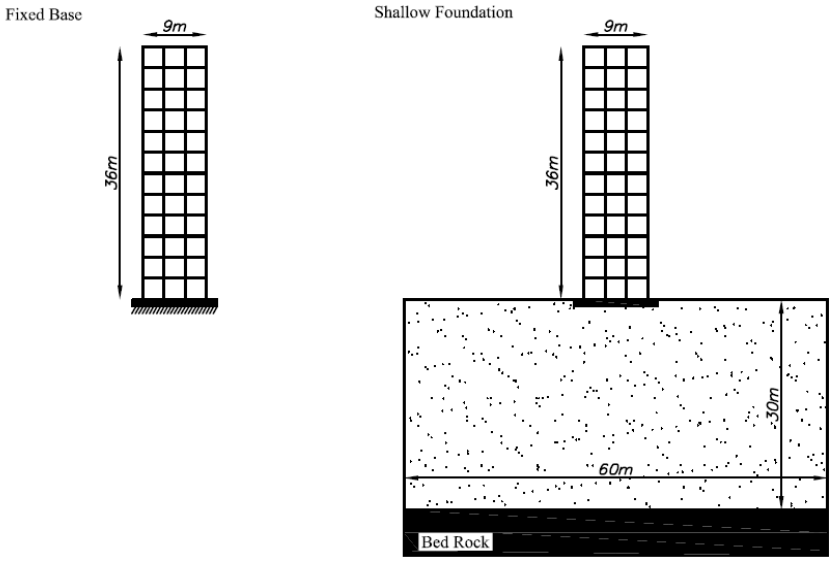

Figure 14. 12-storey steel structure with the fixed-base foundation and shallow foundation

maximum acceleration transmitted to the soil surface increases with increasing the thickness of the soil profile from 10 to 70 m. The maximum increase in acceleration occurs at a depth of 30 m. As a result, considering the thickness of 30 m of soil in soil-structure interaction analyses is a reasonable assumption.

The preliminary analysis of the structure was first performed in ETABS software. The design in ETABS was done in such a way that the stress ratio in beams was less than 0.8 and more than 0.6, and in columns, it was less than 0.4. The dead load and the live load of the floors were considered at 600 and 200 kg/m^2, respectively.

A mat foundation with dimensions of 12x12x1m was considered in numerical analyses. ABAQUS software was used for numerical modeling of soil-structure interaction. The damping of the structure was selected as Rayleigh type, and the damping value was considered at 5%. The damping coefficients were calculated using the frequency of the first and second modes, which are shown in Table 2. The beam and column elements were selected as the second-order one-dimensional element type, and the foundation and soil elements were selected as the Serendipity quadratic type. The sections used for beams and columns in 6-, 9- and 12- storey structures are shown in Table 3.

Von Mises constitutive model with isotropic hardening was selected for steel, and the damaged plasticity model was chosen for concrete. The concrete damage plasticity model is one of the most widely used constitutive models for concrete simulation in ABAQUS software, which has been used in various articles [7]. This model simulates the mechanism of failure in tension and compression in a continuum space using the damage parameter, which is a function of non-elastic strain.

TABLE 2. Rayleigh coefficient for steel structures

Name	Frequency of the first mode	Frequency of the second mode	α	β
S6	0.966	2.930	0.456	0.004
S9	0.836	2.201	0.380	0.005
S12	0.702	2.068	0.329	0.006

TABLE 3. Typical sections of 6,9 and 12-storey structures

Number of stories	Levels	Beam section	Column section
6	1-3	IPE220	Box 220x16mm
	4-6	IPE200	Box 200x16mm
9	1-3	IPE270	Box 280x16mm
	4-6	IPE240	Box 240x16mm
	7-9	IPE200	Box 200x16mm
12	1-4	IPE300	Box 300x16mm
	5-8	IPE270	Box 280x16mm
	9-12	IPE240	Box 240x16mm

The value of the internal dilation angle for concrete is obtained by fitting the model results to laboratory data, which are usually assumed to be between 30 and 40 degrees [18]. The values of the parameters used for concrete and steel are shown in Tables 4 and 5.

The properties considered for the soil are effective in the modeling of soil-structure interaction. The interaction between soil and structure decreases with increasing the stiffness of the soil. The properties of soft clay are selected from real geotechnical explorations, which are

shown in Table 6. The constitutive model used for soil is the Mohr-Coulomb model. Due to the difference between the rock layer and the soft soil in terms of stiffness, the elastic behavior for the rock layer is used, which is shown in Table 7.

The elastic modulus of the rock is 100 times the elastic modulus of the soil. Numerical modeling was performed to examine the effect of thickness, length, and position of the rock layer in soft soil. Therefore, three thicknesses of 1.5, 3, and 6m and four lengths of 7.5, 15, 30, and 60 m were considered for the rock layer. Soft soil was divided into three parts, including upper, middle, and lower, with a thickness of 10 m, and the rock layer was placed at 8, 16, and 24 m depths.

TABLE 4. Constitutive parameters of concrete

Parameter	Value
Mass density	$\rho(kg/m^3)=2350$
Poisson's ratio	$\nu=0.3$
Elastic modulus	$E(MPa)=28284$
Compressive strength	$f_c'(MPa)=32$
Tensile strength	$f_t'(MPa)=3.4$
Dilation angle	31
Eccentricity	0.1
The ratio of initial equibiaxial compressive yield stress to initial uniaxial compressive yield stress	$\sigma_{b0}/\sigma_{c0}=1.16$
The ratio of the second stress invariant on the tensile meridian	$K_c=0.67$

TABLE 5. Constitutive parameters of steel

Parameter	Value
Mass density	$\rho(kg/m^3)=7850$
Poisson's ratio	$\nu=0.3$
Elastic modulus	$E(GPa)=200$
Yield stress	$f_y(MPa)=280$

TABLE 6. Constitutive parameters of the soft soil

Parameter	Value
mass density	$\rho(kPa)=1550$
Poisson's ratio	$\nu=0.4$
Elastic modulus	$E_{\max}(kPa)=7.5e4$
Shear wave velocity	$V_s(m/s)=131$
Cohesion	$c(kPa)=100$
Angle of internal friction	$\phi=14$
Plastic index	$PI=16$

TABLE 7. Constitutive parameters of the rock layer

Parameter	Value
Mass density	$\rho(kPa)=2600$
Poisson's ratio	$\nu=0.25$
Elastic modulus	$E(kPa)=7.5e6$

Considering a large distance between the lateral boundaries of the numerical model increases the computational effort, but the model's width should not be selected so small as to lead to a computational error. In previous studies, it has been recommended to consider the model's width 3 to 5 times the frame width. Rayhani and El Naggar [16] showed that increasing the distance of a boundary from five times the width of the structure to ten times the width has a small effect (5% change) on the seismic response of the models.

An important issue to consider in soil-structure interaction problems is the way of modeling the lateral boundary condition. Lateral boundary conditions must be defined in such a way that waves reaching the lateral boundaries can cross the boundaries. If the waves reaching the lateral boundaries are reflected in the model, they will cause modeling errors. There are different methods for modeling boundaries. The first research in this area was presented by Lysmer and Kuhlemeyer [19]. These authors suggested that boundaries have been modeled as energy absorbers or viscous boundaries. Zienkiewicz et al. [17] proposed the free field boundary model and the lateral boundary model with tied degrees of freedom. Li et al. [20] compared different lateral boundary conditions for soil-structure interaction models. The results showed that if the viscous-spring (VS) boundary condition is used, the small model cannot be used to investigate the interaction. However, the tied degrees of freedom (TDOF) boundary conditions model the interaction with good performance, and the model's size can be considered up to 6 times smaller. In this paper, the condition of the lateral boundary with tied degrees of freedom and the width of 60 m for soil was used to model the problem of soil-structure interaction. The boundary condition of the lower part of the soil layer is defined in such a way that the movement of the soil relative to the bedrock is zero.

Damping in the structure was considered constant (5%) during the analysis. However, damping and shear modulus depend on the value of the shear strain. It is observed that with increasing shear strain, the damping increases and the shear modulus decreases. A study

conducted by Sun et al. [21] was used to model a decrease in shear strength and an increase in soil damping due to the earthquake. By examining laboratory data, Sun et al. [21] showed that changes in shear modulus depend on confining pressure, consolidation history, loading frequency, plasticity, and porosity. Soil plasticity was introduced as the most important factor affecting the change of shear modulus during earthquake loading. These authors presented five curves for different ranges of the plastic index. In this paper, the curve for the plastic index in the range of 10 to 20 was used, as shown in Figures 15 and 16. The equivalent linear method was used to estimate the value of shear modulus and damping. In this method, a linear analysis with initial shear modulus and damping is performed. Then, based on shear strain value, shear modulus value and damping coefficient are estimated.

The contact surface between soil and foundation or between soil and rock has been modeled in the form of traction/separation laws using the Mohr-Coulomb criterion and considering normal and tangential stiffness.

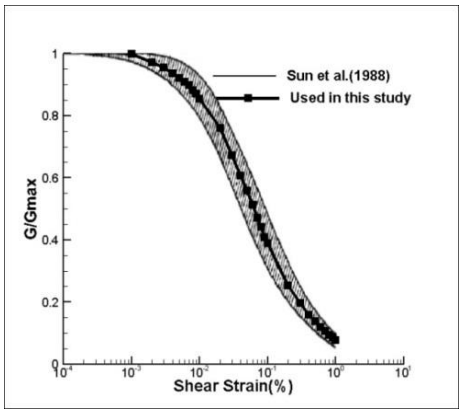

Figure 15. Relationships between G/Gmax and cyclic shear strain

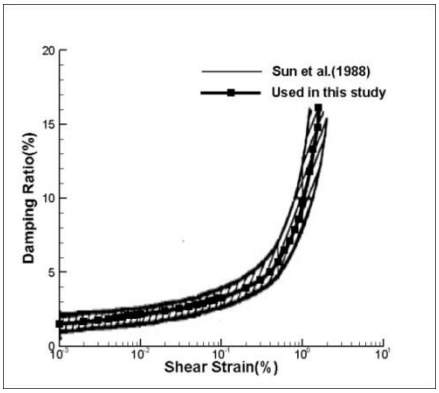

Figure 16. Relationships between the material damping ratio and cyclic shear strain

In this model, the friction is inactive until the adhesion is reduced. If the adhesion decreases, the friction model is activated and contributes to the shear strength. Before the onset of damage, the shear strength is the combination of adhesion and friction. After damage, the adhesion participation is zero, and the shear strength is entirely due to the frictional resistance. Previous studies have recommended that the maximum value of normal and shear stiffness be estimated using the following equation [8, 16].

$$k_n(\max) = k_s(\max) = 10 \times \max\left(\frac{K + 4/3G}{\Delta z_{\min}}\right) \quad (1)$$

In this equation, K and G are the bulk and shear modulus. $\Delta z_{\min}$ is the smallest width of an adjoining zone in the normal direction. The value of contact surface stiffness was considered constant during the analysis. K_n and K_s values for soft clay were selected at $1.07 \times 10^5 kPa/m$. Selecting lower values led to higher estimates of lateral deformation, and higher values did not affect lateral deformation.

4. NUMERICAL SIMULATIONS

Two earthquake records were applied to each of the studied frames. The normal and shear stress contours of 9 storey structure are presented in Figures 17-19 as an example. These figures are obtained by applying the Kobe earthquake. Factors influencing the choice of the earthquake are the intensity, duration, and frequency of the earthquake. The Kobe earthquake is considered in the category of near-field earthquakes, and the El Centro earthquake is considered in the classification of far-field earthquakes. These records have been used in various references to study the interaction of soil and structure. The magnitude of the Kobe earthquake was 6.8, and the magnitude of the El Centro earthquake was 6.9 [22]. Based on the earthquake record, the dominant period of the Kobe earthquake is 0.36, and the dominant period of the El Centro earthquake is 0.56 (Table 8). Figures 20 and 21 show the acceleration records of the El Centro and Kobe earthquakes.

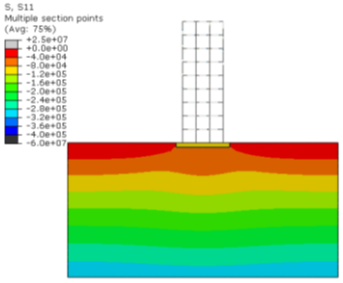

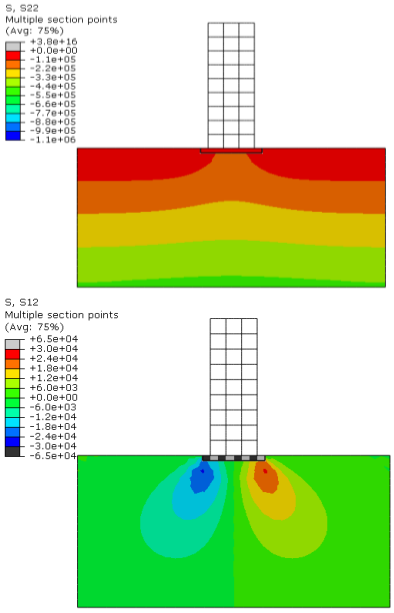

Figure 17. The distribution of normal and shear stress after static analysis

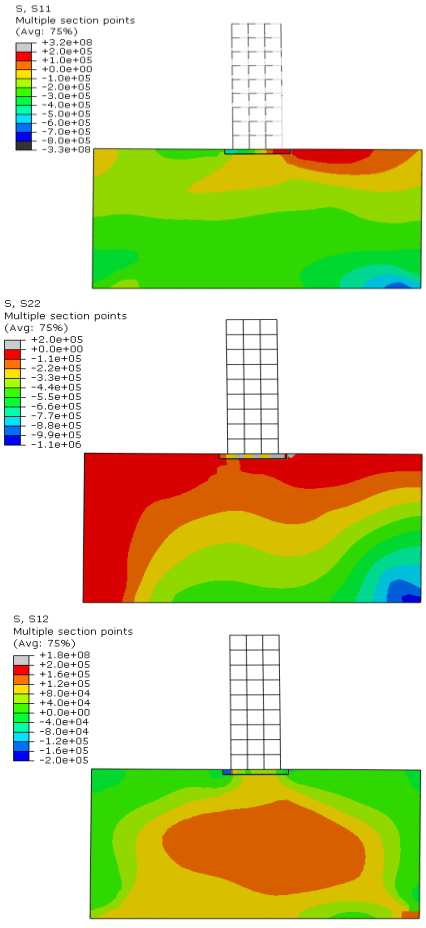

Figure 18. The distribution of normal and shear stress at 4s after beginning of the earthquake

TABLE 8. Ground motion parameters

Parameter	Kobe	El Centro
Magnitude of earthquake	6.8	6.9
Maximum horizontal acceleration	0.834g	0.349g
Predominant period(s)	0.36	0.56
Significant duration(s)	8.4	24.58
Arias intensity(m/s)	8.389	1.758

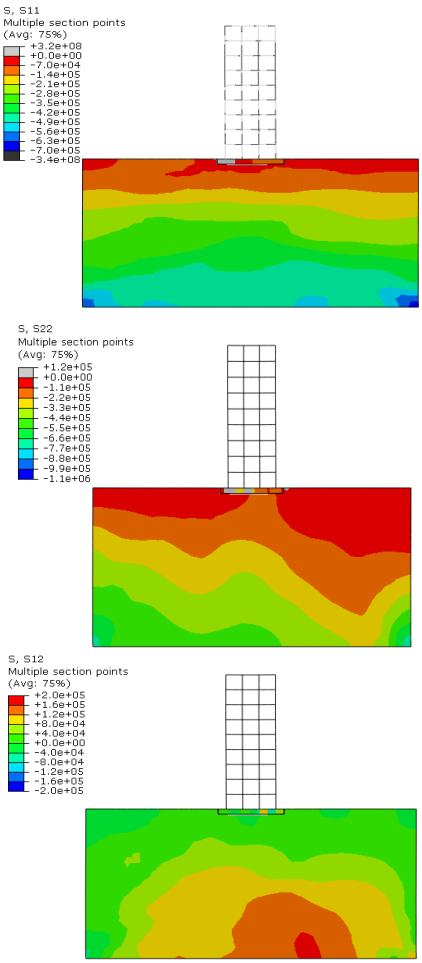

Figure 19. The distribution of normal and shear stress at 8s after beginning of the earthquake

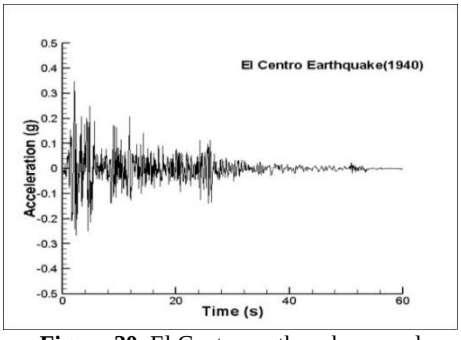

Figure 20. El Centro earthquake record

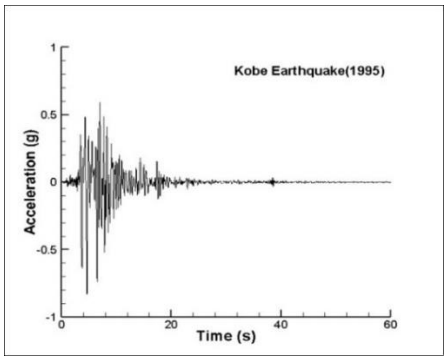

Figure 21. Kobe earthquake record

After analyzing the value of axial force, moment, shear force, base shear, and lateral displacement in the stories were calculated. The mentioned parameters were obtained from the modeling during the time history of the earthquake. The maximum value obtained for each parameter is recorded and investigated in this study. The shear force created in the j-th column of the storey i is displayed by v_j^i. Shear, moment, and axial force created in the 1st column of the storey 15, are shown in Figures 22-24. Displacement and acceleration history at the 15th storey are shown in Figures 25 and 26. The result shows

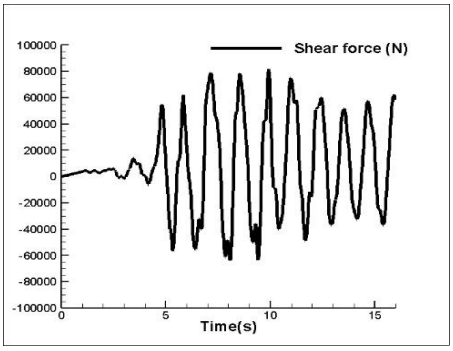

Figure 22. Shear force history in a 1-th column of the storey 15

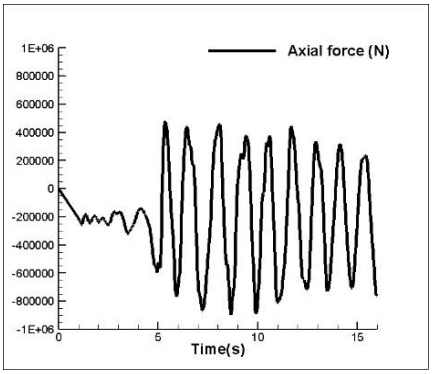

Figure 23. Axial force history in a 1-th column of the storey 15

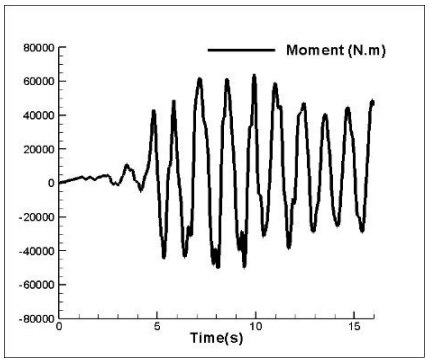

Figure 24. Moment history in a 1-th column of the storey 15

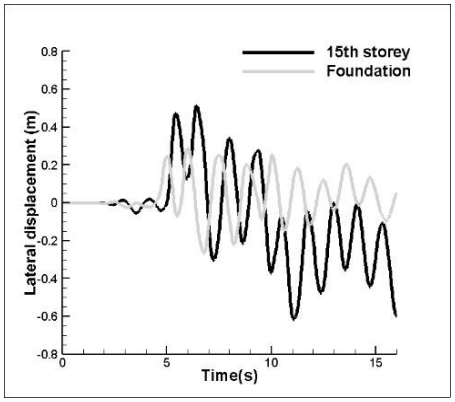

Figure 25. Displacement history at the 15th storey and foundation

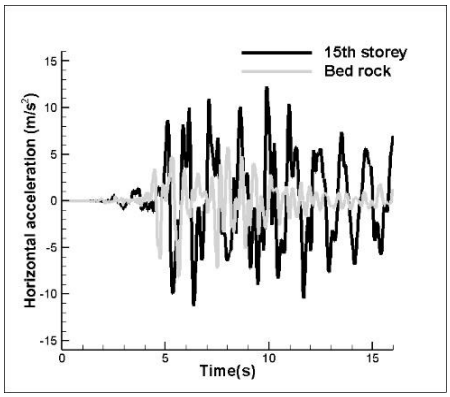

Figure 26. Acceleration history at the 15th storey and bed rock

that the acceleration transmitted to the structure increases. Since; there are four columns in each storey of the structure, the value of j varies from 1 to 4. The maximum value of shear force created in the columns of the storey is recorded and displayed with a parameter $v_{\max}^i$. The mean and maximum values of the parameter $v_{\max}^i$ are displayed with $\bar{V}$ and $V_{\max}$, respectively (Figures 27 and 28).

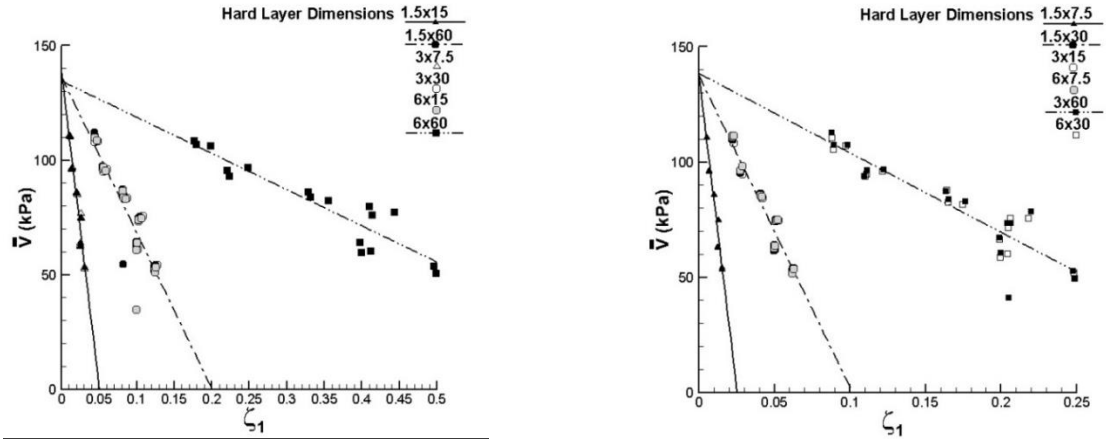

Figure 27. Average shear force of the columns $\bar{V}$

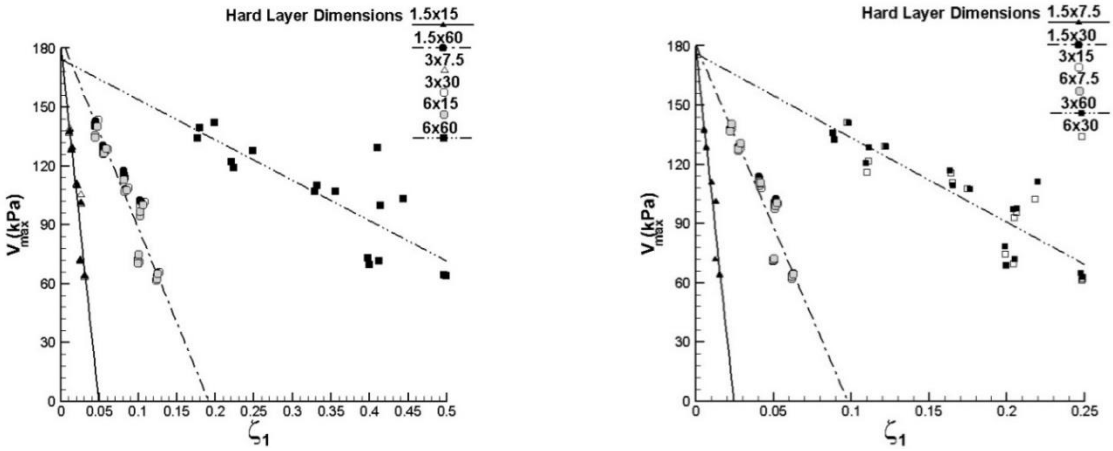

Figure 28. Maximum shear force of the columns $V_{\max}$

$$v_{\max}^{i} = \max(v_j^i) \tag{2}$$

$$\bar{V} = \frac{\sum_{i=1}^{n} v_{\max}^{i}}{n} \tag{3}$$

$$V_{\max} = \max(v_{\max}^{i}) \tag{4}$$

In the above formula, n is the number of stories of the structure.

Similarly, for the moment created in the column of stories, two parameters of $\bar{M}$ and $M_{\max}$ have been defined (Figures 29 and 30), for the axial force, two parameters of $\bar{P}$ and $P_{\max}$ have been defined (Figures 31 and 32), for the lateral displacement of stories, the parameter of $\Delta_{h(\max)}$ has been defined (Figure 33), and for the relative vertical displacement of foundation, the parameter Δ_v (Figure 34) has been defined. Since; the base shear value is considered an important parameter in seismic analysis, two parameters of $\bar{V}_t$ and $V_{t(\max)}$ (Figures 35 and 36) have been used, which are calculated in the following formula.

$$\bar{V}_t = \frac{\sum_{i=1}^{n} \max\left(\sum_{j=1}^{4} v_j^i\right)}{n} \tag{5}$$

$$V_{t(\max)} = \max\left(\max\left(\sum_{j=1}^{3} v_j^i\right)\right) \tag{6}$$

The rock layer dimensions for one parameter are plotted in two diagrams to make the diagrams more straightforward. Dimensions 7.5 x 1.5, 30 x 1.5, 15 x 3, 7.5 x 6, 60 x 3, 30 x 6 (m) are shown in one diagram, and the rest of the size of rock layers is shown in another diagram.

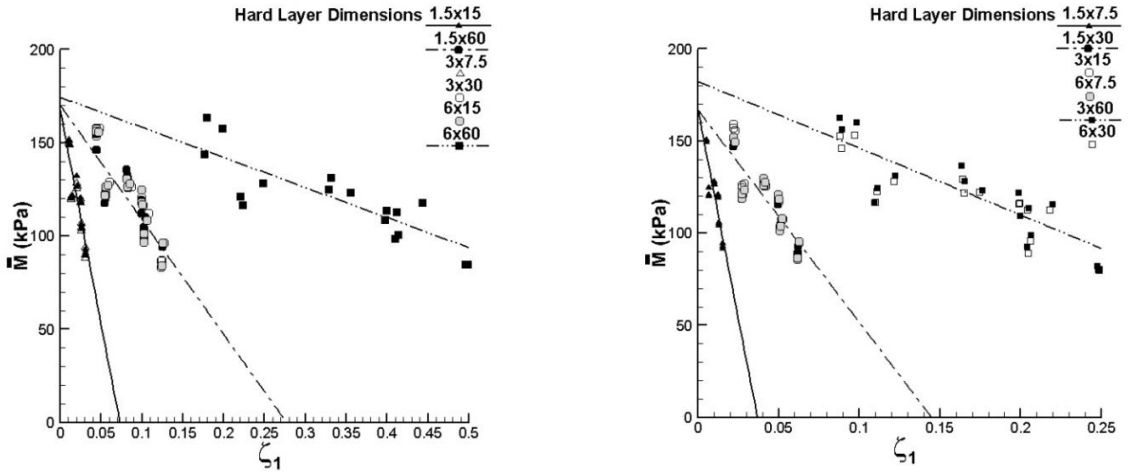

Figure 29. Average moment of the columns $\overline{M}$

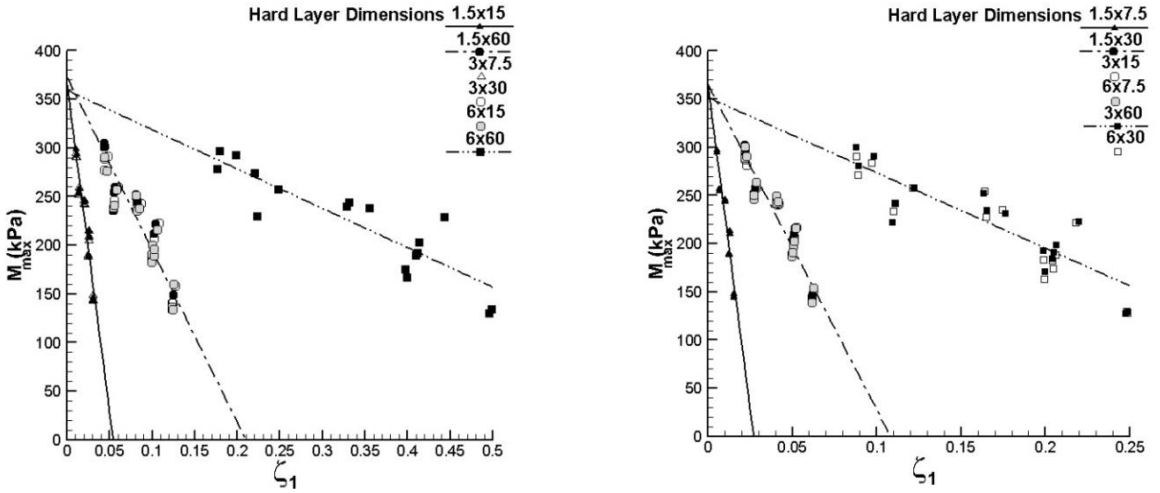

Figure 30. Maximum moment of the columns $M_{\max}$

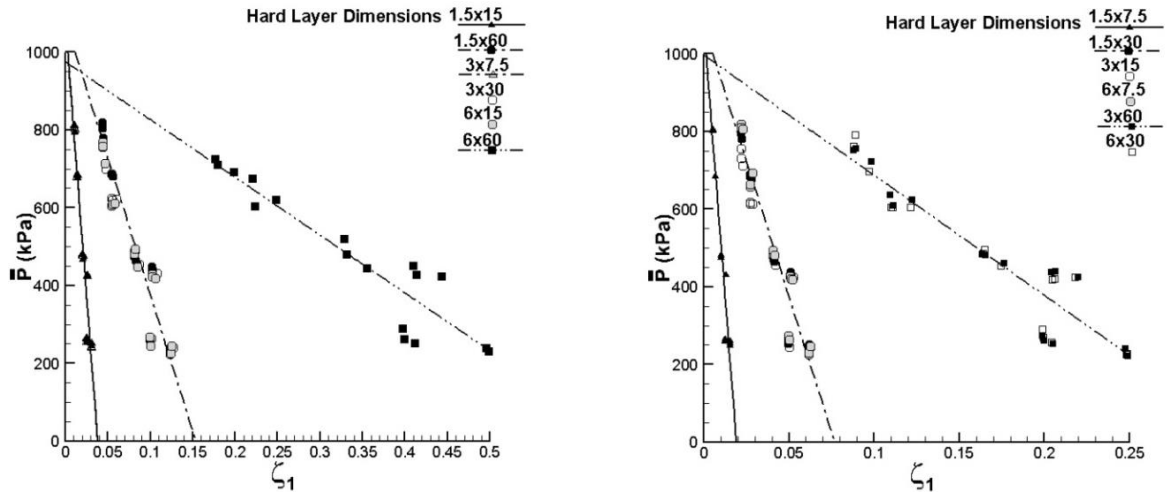

Figure 31. Average axial force of the columns $\overline{P}$

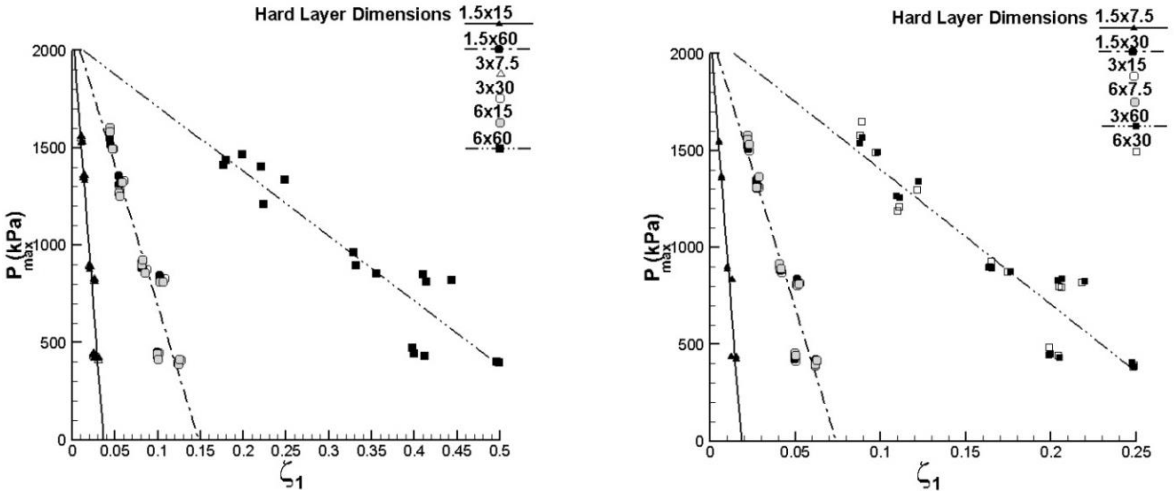

Figure 32. Maximum axial force of the columns $P_{\max}$

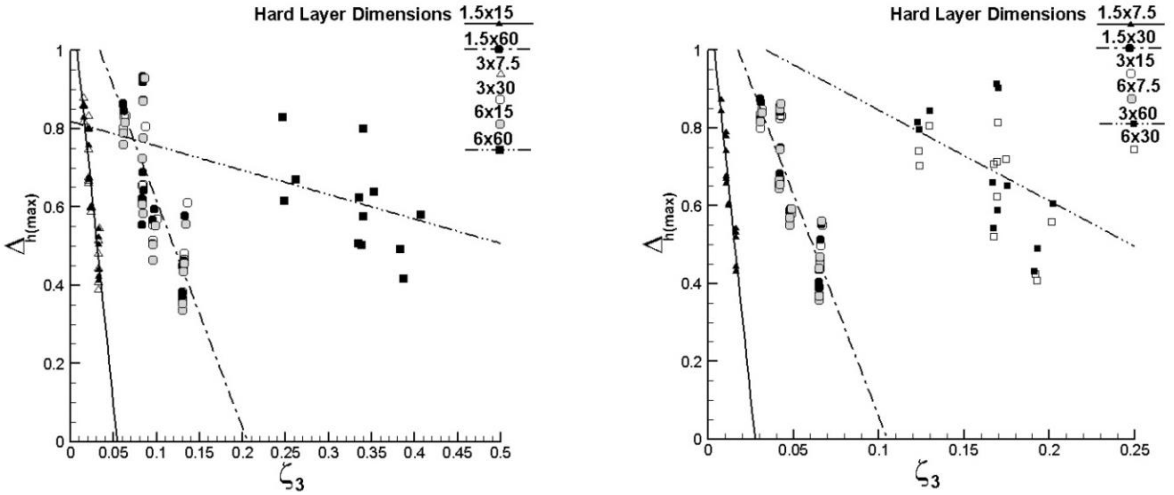

Figure 33. Maximum lateral displacement $\Delta_{h(\max)}$

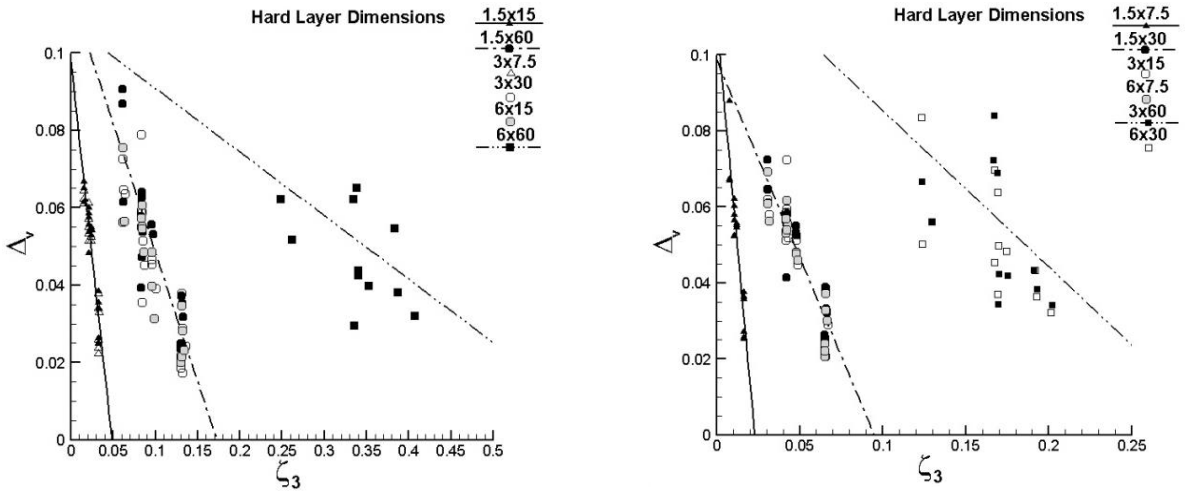

Figure 34. Maximum relative vertical displacement of the foundation Δ_v

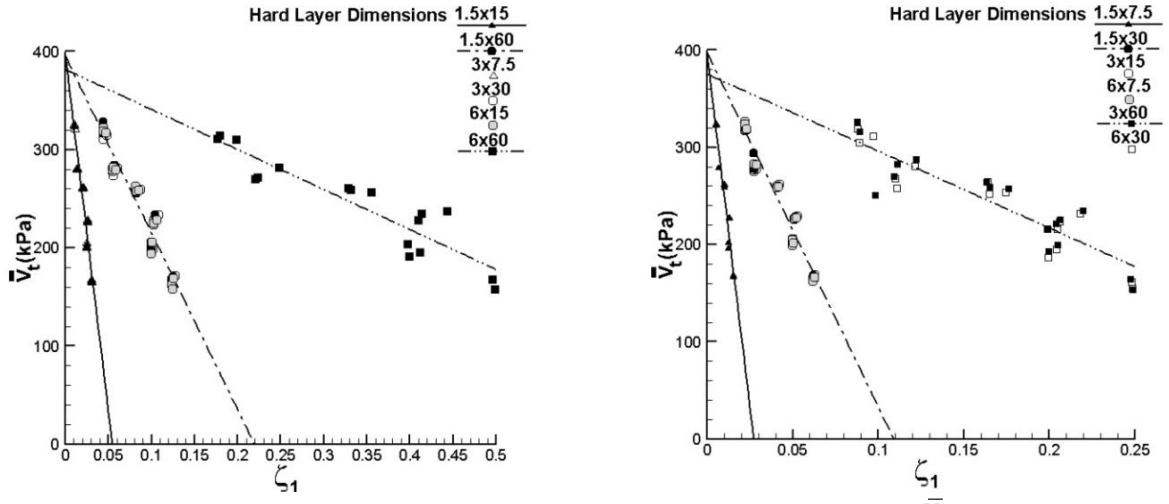

Figure 35. Average of the total shear force of the columns in a storey $\bar{V}_t$

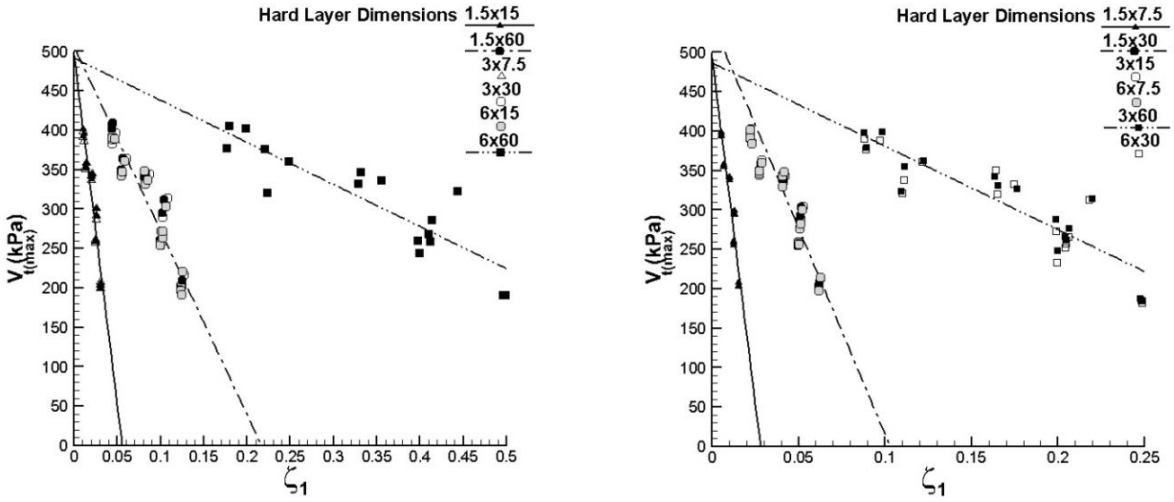

Figure 36. Base shear force $V_{t(\max)}$

In this paper, parameters ξ_1, ξ_3 are introduced to analyze the data. The results showed a correlation coefficient of more than 0.85 with introduced parameters. However, as the mass of the rock layer increases, the data dispersion increases. ξ_1 has been used in force and moment diagrams, and ξ_3 has been used in lateral displacement and relative vertical displacement diagrams.

$$\xi_1 = f_{SS}^2 \times \sqrt{\frac{f_S}{f_E}} \frac{W}{K_S} \tag{7}$$

$$\xi_3 = \frac{f_{SS}}{f_E} \times \frac{W}{K_S} \tag{8}$$

where f_{SS} is the frequency of the soil-structure system, f_S is the frequency of the structure, f_E is the dominant frequency of the earthquake, W is the weight of the rock layer, and K_S is the stiffness of the structure. In estimating the introduced parameters (ξ_1, ξ_3), the values in Tbale 9 are used. The f_S and f_{SS} values were calculated by performing modal analysis in ABAQUS software for each model.

By examining the changes in ξ_1, ξ_3, we can have a better understanding of the effect of the rock layer on the items that are important in the design of structures. One of the important factors affecting the design of structures is the characteristics of the earthquake, which is reflected as the dominant frequency in the ξ_1, ξ_3 parameters. The

TABLE 9. Parameters used in the estimation of ξ_1, ξ_3

Parameter		Value
f_E	Kobe	2.78
	El Centro	1.78
f_S	S6	0.97
	S9	0.84
	S12	0.70
$K_S(N)$	S6	732089
	S9	632903
	S12	700714

Kobe earthquake is a near-field earthquake that has a larger dominant frequency and shorter period than the far-field El Centro earthquake. It should be noted that these earthquakes were selected due to the proximity of magnitude. The magnitude of the El Centro earthquake was 6.9, and the magnitude of the Kobe earthquake was 6.8. Another important factor that should be considered is the frequency of the structure and the frequency of the soil-structure system. If the natural frequency is close to the frequency of the applied force, it is possible for the occurrence of a resonance phenomenon. In the numerical simulation of this paper, the structure and the soil-structure system frequency was less than the dominant frequency of the earthquake, so the f_S / f_E ratio varies between 0.25 and 0.5. The value of the f_{SS} varies between 0.51 and 0.74.

Figures 27 to 36 show that the forces and deformations obtained for rock layers of the same mass (or dimensions) are closely and linearly related to the ξ_1, ξ_3 parameters. In other words, the thickness of the rock layer alone does not affect the interaction of soil and structure, and the length of the rock layer also affects the behavior of the structure and soil. For example, the value of force- obtained for the rock layer in the dimensions of 30 x 1.5, 15 x 3, 7.5 x 6(m) with a good approximation are related linearly to ξ_1. This issue indicates that the presence of a rock layer with a thickness of more than 3 is not necessarily more conservative than a rock layer with a thickness of 1.5 m. In some cases, it can provide worse conditions in terms of force and displacement.

Based on Figures 27 to 36, it can be seen that if the size of the rock layer is constant, if the ξ_1 and ξ_3 value decrease, due to the linear relationship of force with ξ_1 and displacement with ξ_3, the force and displacement caused by the earthquake will increase. For example, since the dominant frequency of the Kobe earthquake is greater than the dominant frequency of the El Centro earthquake, ξ_1 and ξ_3 decrease if the other parameters are constant. As a result, the force and displacement caused by the Kobe earthquake will be greater than that of the El Centro earthquake.

Tables 10 and 11 show the maximum and minimum effect of the presence of a rock layer on the value of force and displacement. In the case of the presence of a rock layer, the mean and maximum axial force is 1.1 times compared to the homogeneous layer of soft clay (from now on, called the reference state).

TABLE 10. Ratios of force and moment relative to the reference value

Record			$\frac{V_{t(\max)}}{V_{t(ref)}}$	$\frac{\overline{V}_t}{\overline{V}_{t(ref)}}$	$\frac{V_{\max}}{V_{\max(ref)}}$	$\frac{\overline{V}}{\overline{V}_{ref}}$	$\frac{M_{\max}}{M_{\max(ref)}}$	$\frac{\overline{M}}{\overline{M}_{ref}}$	$\frac{P_{\max}}{P_{\max(ref)}}$	$\frac{\overline{P}}{\overline{P}_{ref}}$
S6	Kobe	Maximum	1.11	1.07	0.96	0.94	1.05	1.03	1.10	1.10
		Minimum	0.90	0.92	1.06	1.02	0.86	0.90	0.94	0.93
	El Centro	Maximum	1.15	1.06	0.95	0.93	1.19	1.11	1.03	1.03
		Minimum	0.91	0.92	1.06	1.02	0.88	0.88	0.90	0.87
S9	Kobe	Maximum	1.03	1.01	0.96	0.95	1.03	1.07	1.07	1.08
		Minimum	0.95	0.96	1.27	1.06	0.93	0.95	0.95	0.93
	El Centro	Maximum	1.08	1.04	0.92	0.95	1.07	1.12	1.01	1.03
		Minimum	0.86	0.95	1.05	1.02	0.82	0.84	0.96	0.96
S12	Kobe	Maximum	1.04	1.02	0.97	0.95	1.03	1.09	1.03	1.02
		Minimum	0.95	0.77	1.02	1.02	0.92	0.96	0.95	0.86
	El Centro	Maximum	1.06	1.06	0.90	0.97	1.07	1.09	1.00	1.01
		Minimum	0.90	0.93	1.09	1.06	0.87	0.97	0.88	0.88

TABLE 11. Ratios of displacement relative to the reference value

Record			$\frac{\Delta_v}{\Delta_{v(ref)}}$	$\frac{\Delta_{h(\max)}}{\Delta_{h(\max)(ref)}}$
S6	Kobe	Maximum	1.59	1.07
		Minimum	0.56	0.75
	El Centro	Maximum	1.01	1.20
		Minimum	0.56	0.73
S9	Kobe	Maximum	1.15	1.31
		Minimum	0.67	0.65
	El Centro	Maximum	1.04	1.27
		Minimum	0.64	0.76
S12	Kobe	Maximum	1.56	1.02
		Minimum	0.73	0.71
	El Centro	Maximum	0.98	1.00
		Minimum	0.55	0.67

The maximum axial force is related to the rock layer with dimensions of 30 x 6, which is located at a depth of 24 m. The minimum value of the axial force is 0.86 of the reference state and is related to the 60x6 rock layer, which is located at a depth of 8 m. For other parameters, similar information is given in Tables 10 and 11. As can be seen, the value of axial force with a thickness of 1.5 m is between the maximum and minimum value, indicating that the assumption of the presence of a rock layer with less thickness is not necessarily reliable.

The presence of a rock layer causes the maximum axial force to increase by 1.1, the shear force to increase by 1.27, and the moment force to increase by 1.19 compared to the reference state.

Increasing the value of maximum forces indicates that there is a possibility of failure of structural members. The largest increase is related to the shear force. The mean axial force increased by 1.1, the shear force increased by 1.06, and the moment increased by 1.12 compared to the reference state. Since; the mean force and moment value can be considered as a criterion for estimating the construction cost, it has been considered in this paper. The construction cost increases with increasing the mean force and moment. The maximum difference of 12% shows that with optimal design, the cost of constructing the structure will not increase much. It should be noted that there are conditions in which the rock layer reduces the force and moment. The positive effect of the presence of the rock layer on the value of force and moment is a maximum of 18%. Its effect on the mean value of force and moment is 16%.

The value of base shear force with the $V_{t(\max)}$ is shown in Table 10. The presence of a 60 x 6 rock layer, which is located at a depth of 8 m, increases the value of base shear force by 15%. The maximum reducing effect of the presence of the lock layer for the base shear force is 14%, which occurs if there is a 30 x 6 rock layer located at a depth of 24 m. The mean shear force of the storey also varies from 0.77 to 1.07 compared to the reference state. In short, it can be concluded that the presence of a rock layer can increase the value of base shear and the mean shear force of the structure.

The value of horizontal displacement shown in Table 11 indicates that a rock layer with dimensions of 30 x 3(m) located in the middle of the soft soil layer will lead to a 31% increase in lateral displacement caused by the Kobe earthquake. The El Centro earthquake for a rock layer with a dimension of 60x3(m) also causes a 27% increase in lateral displacement. Increased lateral displacement causes the structure's performance to exceed life safety and approach near collapse. In Figures 37 and 38, the relative lateral displacements created in the 9-storey structure are compared in the two cases. As seen, in the presence of a rock layer, for both the Kobe and El

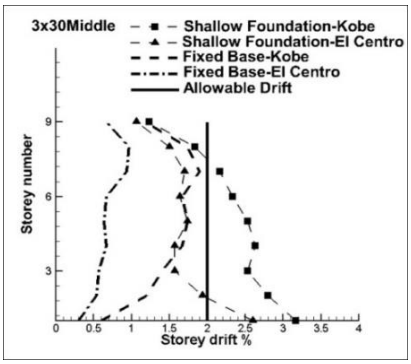

Figure 37. Inter-storey drift Comparison between soil with the rock layer (3x30) and fixed base

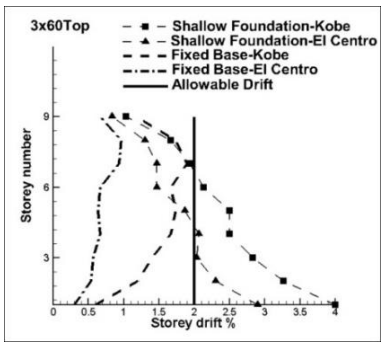

Figure 38. Inter-storey drift Comparison between soil with the rock layer (3x60) and fixed base

Centro earthquakes, the relative lateral displacement has exceeded the value of life safety performance and is close to the collapse level. This condition occurs when the relative lateral displacement with fixed support is within the allowable range.

The maximum value obtained for the relative vertical displacement of the foundation is equal to 1.59 times the reference state and is related to the Kobe earthquake and 60x3(m) rock layer dimensions. This indicates that the presence of a rock layer can also cause the overturning of the structure.

Finally, the statistical study on the dimensions and location of the rock layer and its effect on the maximum force and displacement are shown in Figures 39-42. As seen, 60 x 6(m) dimensions with a distribution of 33% had the greatest effect on increasing, and 30 x 6 dimensions with a distribution of 44% had the greatest effect on decreasing the value of force and moment.

Placement of the rock layer in the last third of the soil layer with a distribution of 61% had the greatest effect on increasing the force and moment, and placement of the rock layer in the middle of soft soil with a distribution of 48% had the greatest effect on reducing the value of force and moment. The area of 180 square meters for the rock layer with a distribution of 64% has the least force and moment, and the area of 360 square meters has the highest value of force and moment. Placement in the upper third of the soil layer with a distribution of 67% has the greatest effect on increasing lateral displacement, and placement in the lower third of the soft soil layer has the greatest effect on reducing lateral displacement.

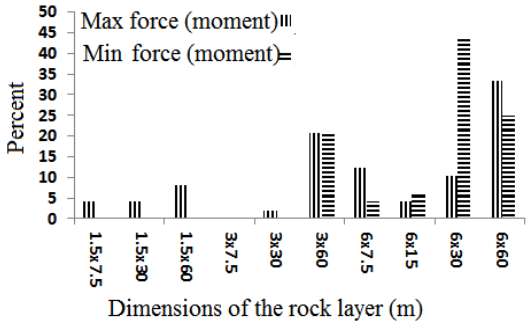

Figure 39. Effect of the rock layer dimension on the force and moment

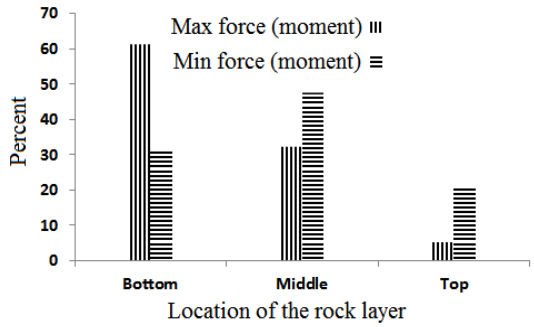

Figure 40. Effect of the rock layer location on the force and moment

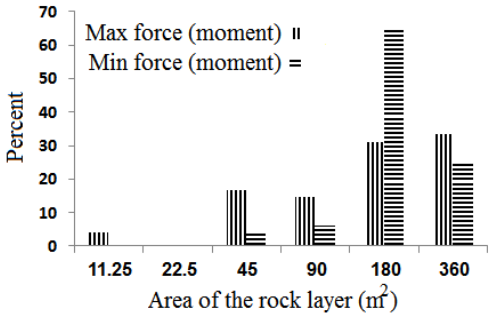

Figure 41. Effect of the rock layer area on the force and moment

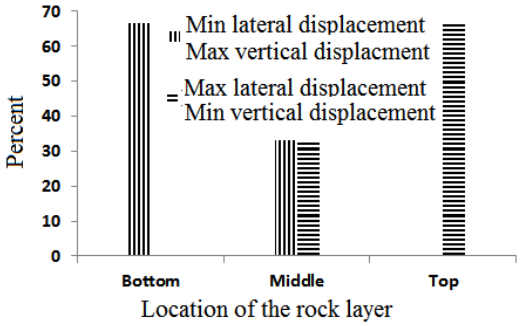

Figure 42. Effect of the rock layer location on the vertcal and lateral displacement

5. CONCLUSION

In this paper, ABAQUS software was used to investigate the effect of a rock layer on the seismic behavior of steel moment frames. In the first step, the shaking table experiment was modeled, and the accuracy of the results was examined. The agreement of the obtained results with the laboratory results shows the accuracy and efficiency of the numerical model. In the next step, three structures of 6-, 9- and 12-storey steel moment frames, which are placed on soft clay, were analyzed. Rock layers with a thickness of 1.5, 3, and 6 m and lengths of 7.5, 15, 30, and 60 m were selected. The elastoplastic constitutive model was selected for soil, steel, and concrete. For the rock layer, the elastic behavior is used. The mean and maximum axial force, shear force, and moment force in the columns were calculated. The obtained results show that the relationship between the force with the introduced parameter ξ_1 and the displacement with parameter ξ_3 is linear. These two parameters depend on the frequency of the structure, the frequency of the soil-

structure system, the dominant frequency of the earthquake, the weight of the rock layer, and the stiffness of the structure. The advantage of using these two parameters is that the location of the rock layer, the height of the structure, and the type of earthquake are specified in the definition of these parameters, and the obtained results can be generalized for other structures and other earthquakes. The results obtained for rock layers with the same weight (or the same dimensions) have a linear relationship with ξ_1 and ξ_3. It reflects the fact that the length of the rock can be as important as the thickness of the rock. As the size of the rock layer increases, the correlation decreases, but the relationship can be considered linear. For rock layers of the same weight, the force and the lateral displacement decrease with increasing ξ_1 and ξ_3. The effect of the rock layer on displacement is more than the force. The presence of a rock layer can increase the maximum value of lateral displacement by up to 31% and the relative vertical displacement of the foundation by up to 59%. Increased lateral displacement causes the performance of the structure to exceed life safety and approach near collapse. The rock layer with dimensions of 60 x 6(m) has the highest value of force (moment), and the rock layer with dimensions of 30 x 6 has the lowest value of force (moment). Placement of the rock layer in the lower third of the soil layer increases the force and reduces lateral displacement, and placement of the rock layer in the middle of the soil reduces the force. Placement of the rock layer in the upper third of the soil increases lateral displacement. The location and dimensions of the rock layer have the most important effect on the force and displacement. The presence of a rock layer can increase the maximum value of axial force, shear force, and moment in the columns of the structure. This suggests that not considering the rock layer in soft soil does not necessarily reliable. The mean value of force and moment increased by a maximum of 12%, which indicates that the cost of construction does not increase significantly with the rock layer.

6. REFERENCES

1. Li, S.-Q. and Liu, H.-B., "Vulnerability prediction model of typical structures considering empirical seismic damage observation data", ***Bulletin of Earthquake Engineering***, (2022), 1-43. doi: 10.1007/s10518-022-01395-y.
2. Li, S.-Q. and Liu, H.-B., "Comparison of vulnerabilities in typical bridges using macroseismic intensity scales", ***Case Studies in Construction Materials***, Vol. 16, (2022), e01094. doi: 10.1016/j.cscm.2022.e01094.
3. Li, S., Chen, Y. and Yu, T., "Comparison of macroseismic-intensity scales by considering empirical observations of structural seismic damage", ***Earthquake Spectra***, Vol. 37, No. 1, (2021), 449-485. doi: 10.1177/8755293020944174.
4. Li, S.-Q., Liu, H.-B. and Chen, Y.-S., "Vulnerability models of brick and wood structures considering empirical seismic damage observations", in Structures, Elsevier. Vol. 34, (2021), 2544-2565.
5. Li, S.-Q. and Liu, H.-B., "Statistical and vulnerability prediction model considering empirical seismic damage to masonry structures", in Structures, Elsevier. Vol. 39, (2022), 147-163.
6. Wolf, J.P., "Dynamic soil structure interaction, PrenticeHall. Inc., Englewood Cliffs, New Jersey, (1985).
7. Bagheri, M., Jamkhaneh, M.E. and Samali, B., "Effect of seismic soil–pile–structure interaction on mid-and high-rise steel buildings resting on a group of pile foundations", ***International Journal of Geomechanics***, Vol. 18, No. 9, (2018), 04018103. doi: 10.1061/(ASCE)GM.1943-5622.0001222.
8. Hokmabadi, A.S., Fatahi, B. and Samali, B., "Assessment of soil–pile–structure interaction influencing seismic response of mid-rise buildings sitting on floating pile foundations", ***Computers and Geotechnics***, Vol. 55, (2014), 172-186. doi: 10.1016/j.compgeo.2013.08.011.
9. Mulliken, J.S. and Karabalis, D.L., "Discrete model for dynamic through-the-soil coupling of 3-d foundations and structures", ***Earthquake Engineering & Structural Dynamics***, Vol. 27, No. 7, (1998), 687-710. doi: 10.1002/ (SICI)1096-9845(199807)27:7<687::AID-EQE752>3.0.CO;2-O.
10. Tabatabaiefar, S.H.R., Fatahi, B. and Samali, B., "Numerical and experimental investigations on seismic response of building frames under influence of soil-structure interaction", ***Advances in Structural Engineering***, Vol. 17, No. 1, (2014), 109-130. doi: 10.1260/1369-4332.17.1.109.
11. Kitada, Y., Hirotani, T. and Iguchi, M., "Models test on dynamic structure–structure interaction of nuclear power plant buildings", ***Nuclear Engineering and Design***, Vol. 192, No. 2-3, (1999), 205-216. doi: DOI: 10.1016/S0029-5493(99)00109-0.
12. Aydin, E., Ozturk, B., Bogdanovic, A. and Farsangi, E.N., "Influence of soil-structure interaction (ssi) on optimal design of passive damping devices", in Structures, Elsevier. Vol. 28, (2020), 847-862.
13. Kim, Y.-S. and Roesset, J.M., "Effect of nonlinear soil behavior on inelastic seismic response of a structure", ***International Journal of Geomechanics***, Vol. 4, No. 2, (2004), 104-114. doi: 10.1061/(ASCE)1532-3641(2004)4:2(104).
14. Fatahi, B., Far, H., Sadeghi Hokmabadi, A. and Samali, B., "Significance of bedrock depth in dynamic soil-structure interaction analysis for moment resisting frames", in International Conference on Performance-Based Design in Earthquake Geotechnical Engineering, Associazione Geotecnica Italiana-Roma., (2012).
15. Holzer, T.L., Bennett, M.J., Ponti, D.J. and Tinsley III, J.C., "Liquefaction and soil failure during 1994 northridge earthquake", ***Journal of Geotechnical and Geoenvironmental Engineering***, Vol. 125, No. 6, (1999), 438-452. doi: 10.1061/(ASCE)1090-0241(1999)125:6(438).
16. Rayhani, M. and El Naggar, M.H., "Numerical modeling of seismic response of rigid foundation on soft soil", ***International Journal of Geomechanics***, Vol. 8, No. 6, (2008), 336-346. doi: 10.1061/(ASCE)1532-3641(2008)8:6(336).
17. Zienkiewicz, O., Bicanic, N. and Shen, F., Earthquake input definition and the trasmitting boundary conditions, in Advances in computational nonlinear mechanics. 1989, Springer.109-138.
18. Jankowiak, T. and Lodygowski, T., "Identification of parameters of concrete damage plasticity constitutive model", ***Foundations of Civil and Environmental Engineering***, Vol. 6, No. 1, (2005), 53-69.
19. Lysmer, J. and Kuhlemeyer, R.L., "Finite dynamic model for infinite media", ***Journal of the Engineering Mechanics***

Division, Vol. 95, No. 4, (1969), 859-877. doi: 10.1061/JMCEA3.0001144.

20. Li, Y., Zhao, M., Xu, C.-s., Du, X.-l. and Li, Z., "Earthquake input for finite element analysis of soil-structure interaction on rigid bedrock", ***Tunnelling and Underground Space Technology***, Vol. 79, (2018), 250-262. doi: 10.1016/j.tust.2018.05.008.
21. Sun, J.I., Golesorkhi, R. and Seed, H.B., "Dynamic moduli and damping ratios for cohesive soils, Earthquake Engineering Research Center, University of California Berkeley, (1988).
22. PEER, *Peer ground motion database*. 2014, Univ. of California Berkeley, CA.

Persian Abstract

چکیده

در نظرگرفتن لایه‌بندی خاک در بررسی لرزه‌ای سازه‌ها مقوله‌ای مهم و اثرگذاراست. در پژوهش‌های پیشین، وجود لایه‌سنگی درون خاک نرم موردتوجه قرار نگرفته‌است. در مقاله حاضر، تاثیر لایه‌ای از سنگ درون خاک نرم بر نیروها و تغییرمکان‌های بوجودآمده در قاب فولادی خمشی کوتاه و متوسط بررسی می‌شود. از این‌رو محاسبات عددی متعددی بروی ۱۲ نوع اندازه متفاوت لایه‌سنگی در سه عمق مختلف انجام شده‌است. مدل‌های عددی بااستفاده از نرم افزار آباکوس در قالب المان محدود و با لحاظ کردن اثرات متقابل سازه و خاک تحلیل شده‌اند. نتیجه بررسی‌های انجام‌شده نشان می‌دهد که مقدار نیرو و تغییرمکان به فرکانس سازه، فرکانس مجموعه سازه و خاک، فرکانس غالب زلزله، وزن لایه‌سنگی و سختی سازه وابسته هستند. در این مقاله، دو پارامتر جدید به‌نحوی تعریف شده‌اند که رابطه‌ای خطی با نیرو و تغییرمکان داشته باشند. نتایج بدست‌آمده گویای آن‌است که ضخامت و طول لایه‌سنگی بر مقدار نیرو و تغییرمکان اثرگذاراست. علاوه براین، وجود لایه‌ای از سنگ درون خاک ممکن‌است در جهت اطمینان نباشد و موجب افزایش نیروی‌برشی تا ۲۷ درصد، نیروی‌محوری تا ۱۰ درصد و لنگر تا ۱۹ درصد شود. تاثیر وجود لایه‌ی سنگی بر تغییرمکان بیش از نیرواست و موجب افزایش تغییرمکان جانبی تا ۳۱ درصد و تغییرمکان نسبی قائم پی تا ۵۹ درصد می‌شود.